Magmatic Controls on Metal Endowments of Porphyry Cu-Au Deposits

Chiaradia, Massimo

How to cite

CHIARADIA, Massimo. Magmatic Controls on Metal Endowments of Porphyry Cu-Au Deposits. In: Tectonomagmatic Influences on Metallogeny and Hydrothermal Ore Deposits: A Tribute to Jeremy P. Richards (Volume I). Sholeh, A. & Wang, R. (Ed.). [s.l.] : Society of Economic Geologists, 2021. p. 1–16. doi: 10.5382/SP.24.01

This publication URL: https://archive-ouverte.unige.ch/unige:155071
Publication DOI: 10.5382/SP.24.01

SEG Special Publications, no. 24, pp. 1–16

Chapter 1

Magmatic Controls on Metal Endowments of Porphyry Cu-Au Deposits

Massimo Chiaradia†

Department of Earth Sciences, University of Geneva, Rue des Maraîchers 13, 1205-Geneva, Switzerland

Abstract

This overview illustrates the processes controlling magma fertility in the formation of porphyry Cu-Au deposits. Magma fertility means all magmatic parameters (e.g., metal and volatile contents, magma and fluid volumes) that might result in higher amounts of metals, which are exsolvable from the magma. Mantle source processes seem to play a fundamental role in the enrichment of primary melts with H_2O, S, and Cl, all essential ingredients to form porphyry deposits, but do not have a particular role in Cu enrichment.

Cu-rich porphyry Cu-Au deposits (i.e., with Au/Cu ~4×10^{-6}) are associated with large magmatic volumes accumulated in the lower thick crust of continental arcs during long-lived periods of compression in a synsubduction environment. Mineralization occurs after such accumulations have reached significant volumes and is the result of the transfer of hydrous magmas from deep to shallower crustal levels, probably favored by tectonic stress changes.

Au-rich porphyry Cu-Au deposits (i.e., with Au/Cu ~80×10^{-6}) are associated with magmatic systems that have evolved at overall shallower crustal levels and for this reason can be found in geodynamic settings characterized by thinner crust (e.g., island arcs with intermediate crust thickness) and/or in variably extensional settings occurring above a slab-metasomatized mantle (postsubduction setting, extensional synsubduction setting). The six largest Au-rich porphyry Cu-Au deposits (>~1,300 tonnes Au) are associated with variably alkaline magmas, which are typical of postsubduction and/or extensional settings, suggesting a petrogenetic control on the Au-rich nature of these deposits.

Introduction

Porphyry Cu-Au deposits form at convergent margins, either coeval with subduction (Andean-type, synsubduction deposits) or in postsubduction (postcollisional to extensional) settings (Fig. 1; Richards, 2009; Sillitoe, 2010). In these deposits, metals are precipitated from hydrothermal solutions at temperatures ranging from >500° to <300°C (as reviewed by Sillitoe, 2010, and references therein). There are four basic ingredients that are necessary to form porphyry Cu-Au deposits: metals (essentially Cu, Au, Mo), the aqueous hydrothermal fluid, metal ligands (mostly Cl and S), and S as the ionic and/or covalent bonding to form solid sulfide and sulfosalt minerals (e.g., Burnham, 1979).

A large amount of research based on geologic observations, geochemical, and isotopic data as well as geochronology indicates that hydrothermal solutions, and all the ingredients they carry that are essential to form porphyry deposits (i.e., metals, ligands, and S), have a dominant magmatic origin (e.g., Gustafson and Hunt, 1975; Burnham, 1979; Hedenquist and Lowenstern, 1994).

Therefore, studying the petrogenesis and evolution of magmatic rocks associated with porphyry deposits is an essential step to understand how and why these deposits form. From this perspective, research has focused on two main magmatic processes that determine the ability of magmas to form porphyry deposits (e.g., Richards, 2013; Wilkinson, 2013): source processes, which could enrich primary basaltic melts in the above ingredients, and intracrustal evolutionary processes, which could modify the contents of those ingredients during the evolution of the primary basaltic melts to more evolved intermediate-felsic magmas that are those ultimately associated with porphyry deposits.

Although postmagmatic processes are very important in upgrading metal concentrations and changing ore mineralogy, with substantial consequences on deposit exploration and exploitation, this review focuses only on the above-mentioned magmatic processes and discusses parameters that could determine the magmatic fertility for porphyry deposits. Fertility is intended as the combination of magmatic parameters (e.g., metal and volatile contents, magma and fluid volumes) that, being consistent with petrogenetic processes of arc magmatism, might result in higher amounts of metals exsolvable from the magma. Large databases are used (Chiaradia, 2014, 2015) on the geochemistry of convergent margin magmas of recent age (Miocene to Quaternary) and petrologic modeling (Chiaradia and Caricchi, 2017; Chiaradia, 2020a, b) to understand how source and intracrustal magmatic processes can determine the fertility of magmas. This approach eliminates problems related to hydrothermal alteration that almost invariably overprints porphyry-related magmatic systems. Whenever possible, how the geochemical compositions of intrusive rocks of porphyry-related magmatic systems fit in the large dataset of recent arc magmas and their petrologic modeling is shown.

The Mantle Source Role in Generating Porphyry-Fertile Magmas

Porphyry Cu-Au deposits form at convergent plate margins, either coeval with subduction or postsubduction (Richards,

†E-mail: Massimo.Chiaradia@unige.ch

Open Access (CC-BY-NC) publication of the Jeremy P. Richards memorial volume was generously supported by BHP Metals Exploration and the Laurentian University Mineral Exploration Research Centre (MERC) and Harquail School of Earth Sciences (HES).

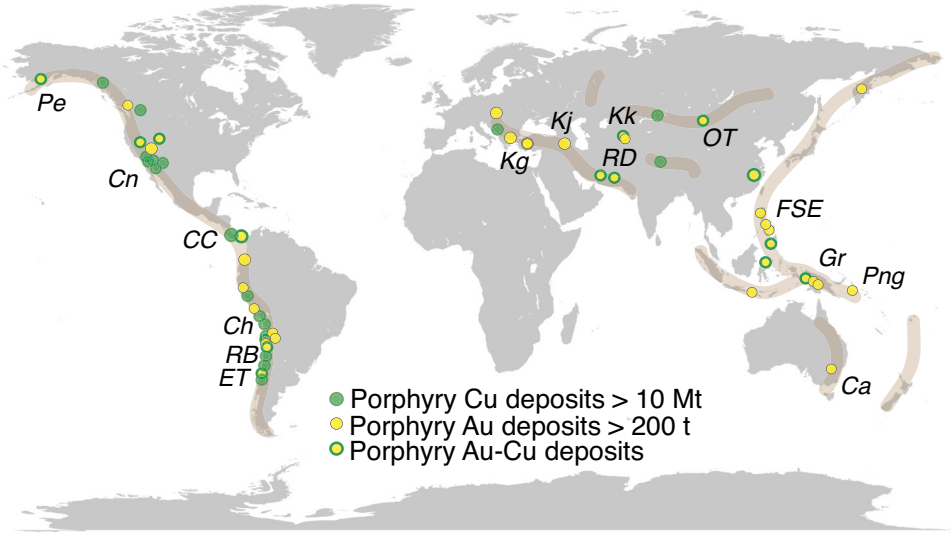

Fig. 1. Worldwide distribution of major porphyry Cu-Au deposits with respect to their metal commodities and endowments (modified after Sillitoe, 2010). Abbreviations: Ca = Cadia, CC = Cerro Colorado, Ch = Chuquicamata, Cn = Cananea, ET = El Teniente, Es = Escondida, FSE = Far South East-Lepanto, Gr = Grasberg, Kg = Kisladag, Kj = Kadjaran, Kk = Kalmakyr, LP = Los Pelambres, OT = Oyu Tolgoi, Pe = Pebble, Png = Panguna, RB = Rio Blanco RD = Reko Diq.

2009). In both cases the source of the primary basaltic melts, from which, subsequently, derivative intermediate to felsic magmas directly associated with porphyry deposits evolve, is a mantle wedge metasomatized by slab-derived fluids. Although the processes of magma generation in the above two settings might differ (Richards, 2009), we can consider primitive arc basalts as the typical example of parents of porphyry-related magmatic systems, because it is agreed that they form from a slab-metasomatized mantle (e.g., Tatsumi, 1989).

Many studies have highlighted the peculiar geochemical characteristics of arc basalts, especially concerning the main ingredients necessary to form porphyry Cu-Au deposits (i.e., metals, H_2O, S, Cl contents). These characteristics are briefly summarized, highlighting differences or similarities between arc basalts and MORB (mid-ocean ridge basalts), as a reference rock that is not associated with porphyry deposits.

Source differences in metal contents

The bulk budget of chalcophile metals (i.e., Cu, Au) in mantle peridotite resides in sulfides, which, depending on pressure and temperature (P-T) conditions, can be either in the solid or liquid form (Audétat and Simon, 2012). Therefore, the contents of these metals in primary basaltic melts issued from partial melting of peridotite is controlled to the largest extent by sulfide solubility into the basaltic melt. It is known that sulfide solubility in silicate melts is strongly dependent, in addition to temperature, pressure, and FeO contents (O'Neill and Mavrogenes, 2002), on f_{O_2} conditions, with higher f_{O_2} conditions favoring higher sulfur solubility and therefore higher metal contents, at equal partial melt fractions (Jugo, 2009).

Remarkably, primitive arc basalts (irrespective of whether they are island or continental arc) have broadly similar average Cu contents (80–100 ppm; Chiaradia, 2014). Even more notable, arc basalts have the same Cu contents as midocean ridge basalts (MORBs; Lee et al., 2012). This has been taken as evidence for similar f_{O_2} conditions in the sub-arc and sub-ridge mantle (Lee et al., 2012), despite widespread belief that arc magmas should be more oxidized than MORBs (e.g., Kelley and Cottrell, 2009). Without entering this ongoing debate, the very similar Cu contents of all arc basalts and MORBs suggest that Cu content of primitive arc basalts is not a main factor in determining the fertility of arc magmas. Thus, other factors associated with arc magmas must play a more prominent role than Cu contents.

Because of analytical challenges, much less information is available for gold contents in primitive arc magmas. Moss et al. (2001) and Jenner et al. (2010) have measured gold contents in melt inclusions of back-arc magmatic rocks (Lau and Manus Basin) and found that they are somewhat higher (4.2–6.2 ppb) than Au contents in MORBs (<1 ppb).

Source differences in H_2O, S, and Cl contents

H_2O contents of primitive arc basalts are quite homogeneous irrespective of the intra-oceanic or continental nature of the arc, and range between 2 and 6 wt % with an average of 3.9 ± 0.4 (1σ) wt % (Plank et al., 2013). There is debate on the actual meaning of such a homogeneous H_2O content. This may be real, indicating a process that systematically leads to primary arc basalts with a restricted range of H_2O contents (Plank et al., 2013). On the other hand, it could be the result of shallow pressure reequilibration of primary arc basalts (Turner and Langmuir, 2015), although this seems to be at odds with geochemical and thermobarometric indications that arc magmas evolve at variably deep levels (Annen et al., 2006; Plank et al., 2013, and references therein).

Primary or primitive arc magmas, and by inference also postsubduction basalts that derive from a slab-metasomatized mantle, are nonetheless much richer in H_2O than MORBs (avg ~0.25 wt %; Wallace, 2005), and this might be one of the main reasons why porphyry-type mineralization is exclusively associated with subduction-related processes (Chiaradia, 2020a; Rezeau and Jagoutz, 2020).

The same holds true for S and Cl. These elements, which are essential for complexing of chalcophile metals in hydrothermal solution and to fix them in sulfide minerals, are significantly more enriched in primary arc basalts (S 900–>3,000 ppm; Cl 500–6,000 ppm; Hattori and Keith, 2001; Wallace, 2005; Aiuppa et al., 2009) than in MORBs (S ~1,100 ppm; Cl <400 ppm; e.g., Wallace, 2005; Aiuppa et al., 2009).

In summary, source processes leading to the formation of primitive arc basalts, the ultimate parents of more evolved intermediate to felsic magmas associated with porphyry deposits, appear to play a more important role in the enrichment of such melts in H_2O, S, and Cl rather than in metals, particularly Cu. Appropriately high contents of volatile species in the primary basalts that are associated with the generation of porphyry deposits seem to be a critical source control on primary magma fertility (e.g., Chiaradia, 2020a; Rezeau and Jagoutz, 2020). This does not discount the potential importance of metal enrichment in magmas (e.g., Keith et al., 1997; Core et al., 2006; Cox et al., 2020) but suggests that the latter is probably not the main variable in determining the formation of most economic porphyry deposits. Nonetheless, it is shown below that magmatic Au enrichment in variably alkaline magmas could be responsible for the formation of the porphyry Cu-Au deposits with large Au endowments.

Interarc differences?

It is known that most major porphyry Cu deposits are found in arcs associated with thick crust (e.g., Sillitoe, 1972; Kesler, 1997). It is therefore important to understand whether such a preferential association derives from source differences in the primary basaltic melts or is due to different intracrustal processes associated with arcs of different thicknesses. As discussed above, there are no evident differences in metal and volatile contents between arcs developed on thick continental crust and those developed on thin oceanic crust, despite the fact that these two types of arcs are often characterized by broadly different slab dips, slab temperatures and ages, and slab descent rates (e.g., Syracuse et al., 2010). This seems to suggest that, whereas the essential ingredients to form porphyry Cu-Au deposits are equally available in thin and thick arcs, the preferential association of porphyry Cu deposits with thick arcs derives from intracrustal processes (see discussion below). Whether and how these are controlled by geodynamic parameters of the subduction zones (slab dips, slab temperatures and ages, and slab descent rates) needs to be investigated. It should be noted, however, that giant porphyry Cu-Au deposits are also found in relatively thin arc settings, like those in the southwest-Pacific Ocean (e.g., Grasberg, Batu Hijau, Ok Tedi, Onto). The occurrence of porphyry Cu-Au deposits in thinner arcs and their relationships with porphyry Cu-Au deposits of thick arcs will be discussed more in detail in a later section.

Intracrustal Magma Evolution Processes in Generating Porphyry-Fertile Magmas

Porphyry deposits are genetically and temporally associated with intermediate to felsic magmas (Sillitoe, 2010, and references therein). Therefore, the evolution of arc basalts to such intermediate-felsic compositions represents an important step in determining the fertility of a magma toward the formation of porphyry deposits.

Large-scale geochemical datasets of recent arc magmatic rocks can be used to evaluate the first-order processes that control magma evolution and geochemical compositions in arcs, and how these processes could influence magma fertility. In order to do this, the evolution in arc magmas of some key major elements (MgO, SiO_2, $Fe_2O_{3(total)}$), Cu, and trace element ratios (Sr/Y) that are used to indicate magma fertility for the formation of Cu-Au porphyry deposits (e.g., Loucks, 2014) are investigated.

Geochemical features of recent magmatic arcs

Arc magmas are characterized by two main sub-alkaline evolutionary trends: tholeiitic and calc-alkaline. The tholeiitic and calc-alkaline trends differ for the extent of $Fe_2O_{3(total)}$ enrichment during magmatic evolution (e.g., with decreasing MgO). Tholeiitic series magmas are characterized by a strong $Fe_2O_{3(total)}$ enrichment at intermediate compositions (MgO values of 4–6 wt %) before subsequent depletion (Miyashiro, 1974). By contrast, calc-alkaline series magmas are characterized by a continuous $Fe_2O_{3(total)}$ depletion throughout the magmatic arc differentiation process.

Discussion is ongoing around the causes of these two distinct trends. It is agreed that the early fractionation of Fe-rich minerals (e.g., magnetite ± garnet ± amphibole) is responsible for the $Fe_2O_{3(total)}$ depletion that is typical of the calc-alkaline trend (e.g., Sisson and Grove, 1993; Tang et al., 2018). However, why this occurs more in some arcs than in others is a matter of debate. Chiaradia (2014) showed that the degree of calc-alkalinity is linearly correlated with the thickness of the crust of the overriding plate, and that there is a continuous transition between tholeiitic and calc-alkaline series (Fig. 2a). This was interpreted as the result of early stabilization of magnetite at high pressure due to higher H_2O contents associated with high-pressure fractionation (Sisson and Grove, 1993). Tang et al. (2018) and Lee and Tang (2020) attributed the Fe depletion in thicker arcs to early garnet fractionation, with garnet being the most Fe-rich mineral fractionating at high pressure. On the other hand, Turner and Langmuir (2015) attributed the relationship between calc-alkalinity and crustal thickness to different degrees of partial melting of the mantle wedge. The latter would correlate with the thickness of the crust of the overriding plate, because a thicker crust results in a deeper location of melting of the mantle wedge (see also Perrin et al., 2018). Therefore, a lower degree of partial melting would occur beneath arcs built on thicker crust. Since H_2O is an incompatible species in magmatic processes, and assuming similar mantle-wedge H_2O contents, this would result in primary basaltic melts being more enriched in H_2O (and other incompatible elements) beneath thick arcs than under thin arcs. Therefore, if this idea is correct, ultimately the occurrence of distinct calc-alkaline and tholeiitic series would be a source process rather than being due to crustal evolution (e.g., Chin et al., 2018).

Regardless of the causes of the association of the calc-alkaline series with thicker arcs and of the tholeiitic series with thinner arcs, it is significant that the average Cu contents in arc magmas follow distinct evolutionary trends that depend on the crustal thickness (Fig. 2b). In particular, in thinner crust, average Cu contents increase from 80 to 100 ppm in basaltic magmas up to ~200 ppm in magmas of intermediate

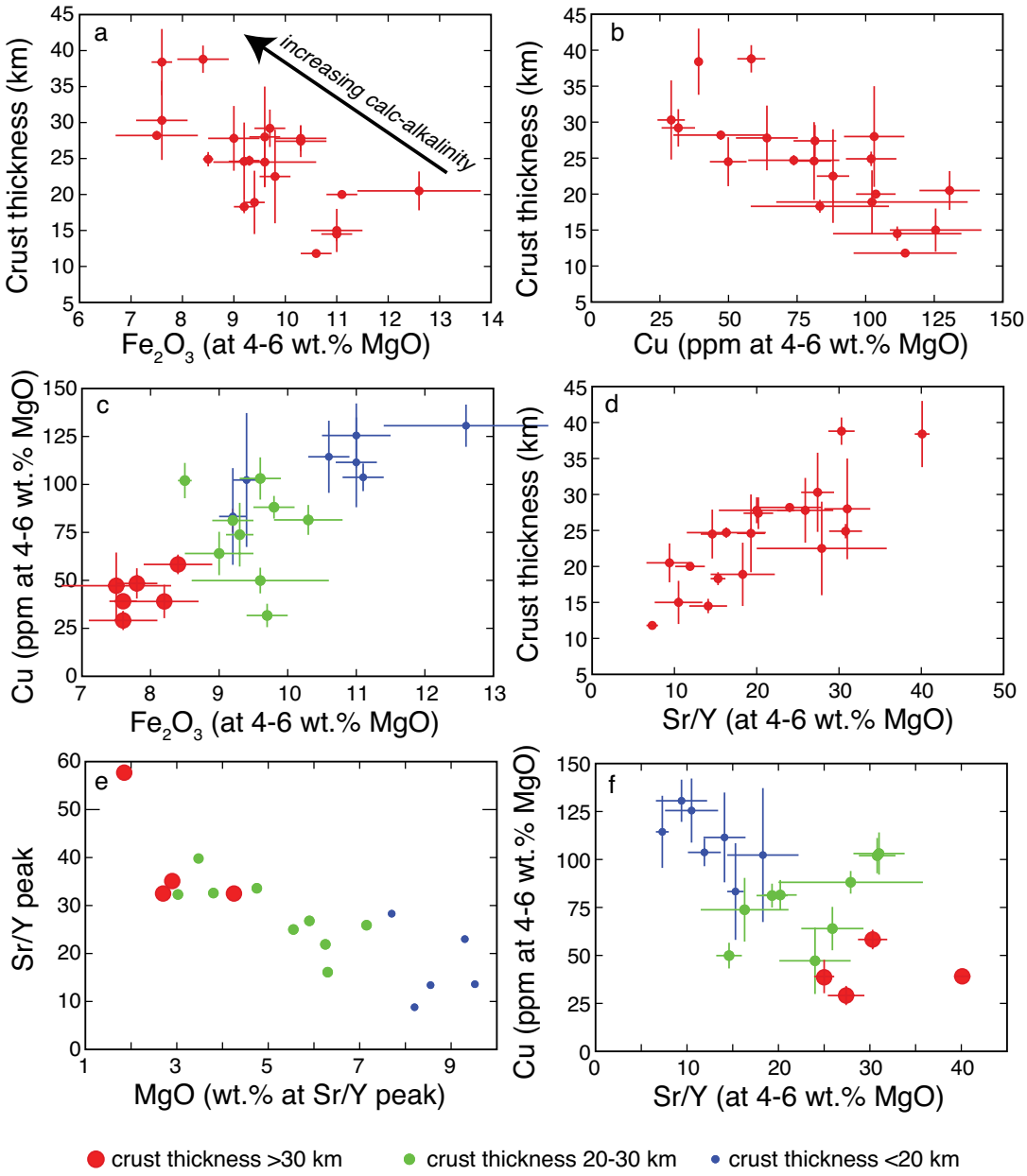

Fig. 2. Systematics of worldwide recent arc magmatic rocks (from data in Chiaradia, 2014, 2015). Each point in panels (a)-(d) and (f) represents individual arc averages of the median Cu, Fe_2O_{3total}, and Sr/Y values comprised between 4 and 6 wt % MgO with associated 1σ uncertainties and average crustal thickness values with associated 1σ uncertainties. Points in panel (e) are peak Sr/Y values from the best-fit exponential functions fitted through the median values in the Sr/Y-MgO space and therefore have no standard deviation values associated. Color and size codes refer to arc thicknesses as indicated in the legend.

compositions (MgO 4–6 wt %) before declining with further evolution (Chiaradia, 2014). Instead, in thick arcs, average Cu values decrease continuously throughout magmatic differentiation (Chiaradia, 2014). As such, Cu displays an identical behavior to $Fe_2O_{3(total)}$ during evolutionary processes of arc magmas, which results in a correlation between these two elements at the global scale (Fig. 2c). The correlation between Cu and $Fe_2O_{3(total)}$ evolutionary trends in arc magmas has been taken as evidence for sulfide saturation induced by magnetite crystallization (Jenner et al., 2010; Chiaradia, 2014). Because, as discussed above, magnetite is an early fractionating phase in hydrous arc magmas of thicker crust, Cu would be more depleted in this environment than in arc magmas of thinner crust, where magnetite crystallization occurs only below MgO values of ~4 wt % (Chiaradia, 2014). An alternative possibility is that sulfide saturation is promoted by magma evolution at deep crustal levels (Matjuschkin et al., 2016), which can only occur in thicker arcs, or by the fractionation of Fe-rich garnet (rather than or in addition to magnetite), which causes Fe depletion (Tang et al., 2018) that would strongly decrease sulfide solubility (e.g., O'Neill and Mavrogenes, 2002). In the latter case, magmatic garnet fractionation occurs in hydrous

magmas at high pressure (>0.8–1.2 GPa: Müntener et al., 2001; Alonso-Perez et al., 2009) and, therefore, again only in a thick crust.

Another geochemical parameter of arc magmas that is worth investigating is the Sr/Y ratio, which may provide insights on the fertility of magmas associated with porphyry Cu-Au deposits (Richards and Kerrich, 2007; Richards, 2011; Loucks, 2014). Loucks (2014) compiled Sr/Y values of magmatic rocks associated with porphyry Cu-Au deposits, demonstrating that Cu-rich porphyry Cu-Au deposits are associated with intrusions that have an average Sr/Y of 100 ± 50 (1σ), whereas Au-rich porphyry Cu-Au deposits are associated with magmatic rocks that have a lower average Sr/Y value of 50 ± 25 (data elaborated in Chiaradia, 2020b). Here and throughout the terms Cu- and Au-rich porphyry Cu-Au deposits are used for deposits with Au/Cu of ~4×10^{-6} and 80×10^{-6}, respectively (see Chiaradia, 2020b, and below).

There has been much debate on the association of porphyry Cu-Au deposits with high Sr/Y intrusions, and its meaning, mostly because of the controversial interpretation of such high Sr/Y values in arc magmas (Richards and Kerrich, 2007 and references therein). High Sr/Y values in magmatic rocks may derive from retention of Y in a refractory source, or in fractionating minerals like garnet and amphibole, and concentration of Sr in partial or residual melts, due to the instability of plagioclase (the main host of Sr in magmatic rocks), again either in the source or as a fractionating mineral. Therefore, high Sr/Y arc magmas are considered to originate through two main distinct processes: (1) a source process where the subducted oceanic slab melts within the garnet stability field and eventually the high Sr/Y melt interacts with the overlying mantle wedge during ascent (Defant and Drummond, 1990); or (2) intracrustal magmatic fractionation of amphibole, garnet ± titanite at high pressure and high P_{H_2O}, eventually accompanied by partial melting and assimilation of lower crustal rocks (MacPherson et al., 2006; Richards and Kerrich, 2007; Chiaradia et al., 2009; Loucks, 2014).

The source process that generates high Sr/Y slab melts might have a metallogenetic potential, in that slab melts are more oxidized than slab fluids, because the melts may be Fe^{3+} dominant, whereas aqueous fluids are Fe^{2+} dominant (Mungall, 2002). The higher oxidation potential of slab melts would promote a more efficient extraction of chalcophile metals from the mantle source, producing higher Cu and Au in primary melts (Mungall, 2002). In reality, it has been shown that the major oxidation agent in subduction zones is sulfate, which is not necessarily more soluble in slab-derived melts than in aqueous fluids (e.g., Bénard et al., 2018). Another metallogenetic factor associated with slab melting would be the direct transfer of high metal contents of the oceanic crust to the subduction-related magmas (Sun et al., 2011), although arc-magma systematics do not show the occurrence, on average, of primary arc basalts with anomalously high Cu contents (Lee et al., 2012; Chiaradia, 2014).

The metallogenetic potential of the intracrustal process that generates high Sr/Y magmas instead has been attributed to the higher H_2O contents that are typically associated with derivative magmas having such a signature (Richards, 2011); their prolonged evolution in the lower to mid-crust would allow the build-up in the magma of the ingredients necessary to form a porphyry deposit (Rohrlach and Loucks, 2005; Chiaradia and Caricchi, 2017; Du and Audétat, 2020).

Chiaradia (2015) has addressed the problem of the meaning of Sr/Y systematics in arc magmas using a large database of recent arc magmatic rocks. In addition to Cu and $Fe_2O_{3(total)}$ (Fig. 2a-c), also Sr/Y values (at MgO 4–6 wt %) vary continuously with the thickness of the overriding plate upon which the arc is constructed (Fig. 2d). At the two end members, arc magmas associated with thin crust display a continuous decrease of Sr/Y values with magmatic differentiation (e.g., decreasing MgO), whereas thick arcs display an increase of Sr/Y values up to MgO values of 2 to 6 wt %, below which Sr/Y values start to decline. The MgO values at which Sr/Y peak values occur change systematically with crustal thickness, trending to lower MgO values as crustal thickness increases (Fig. 2e). All of these correlations provide strong evidence that the Sr/Y arc systematics are controlled by intracrustal magmatic evolution at the global scale. Thicker arcs result in average deeper magmatic evolution, leading to preferential fractionation of Y-bearing minerals (garnet and amphibole) and suppression of Sr-bearing plagioclase. This results in a continuous increase of Sr/Y values from basaltic to intermediate (MgO 2–6 wt %) magmas. In addition, the Sr/Y peak value is systematically shifted to lower MgO values as the crustal thickness increases (Fig. 2e), supporting the argument that, on average, the differentiation of arc magmas occurs at increasingly deeper levels with increasing crustal thickness (see also Farner and Lee, 2017).

In summary, $Fe_2O_{3(total)}$, Cu, and Sr/Y display systematic and continuous changes with thickness of the overriding plate (Fig. 2). $Fe_2O_{3(total)}$ systematics suggests that there is a continuum between the tholeiitic and calc-alkaline series and that the transition from one to the other is controlled by crust thickness (whatever the ultimate reason, whether intracrustal evolution or indirect control of crustal thickness on degree of partial melting of the mantle wedge, as discussed above). Copper systematics is strongly controlled by $Fe_2O_{3(total)}$ behavior, with continuous Cu depletion during calc-alkaline magma differentiation and Cu enrichment during tholeiitic magma differentiation (down to 2–6 wt % MgO). Values of Sr/Y are also controlled by crustal thickness, with a thicker crust, on average, leading to higher Sr/Y values. It follows that increasing Sr/Y values coincide with an increasing calc-alkaline character of the arc magma series and also with decreasing average Cu contents in intermediate arc magmas (Fig. 2f). Since porphyry Cu deposits are typically associated with intermediate calc-alkaline and high Sr/Y magmas from thick arc settings (see above), this again suggests that the Cu content of intermediate-composition magmas associated with porphyry deposits is not the main control on their fertility. Other parameters that are associated with the magma evolution within the calc-alkaline series, and result in high Sr/Y values, are more important than Cu contents.

Why Do Porphyry Deposits Have Different Cu Endowments?

A fundamental question to be addressed when developing genetic models of porphyry Cu deposits is not only why, when, and where they can form, but also why they have large differences in their metal endowments. Indeed, economic

porphyry Cu deposits range in size from a few million metric tonnes (Mt) Cu to >100 Mt and from a few tons (t) to >2,500 t of Au (USGS database: https://mrdata.usgs.gov/porcu/). In the previous sections it has been inferred that intracrustal processes must play an essential role in determining the fertility of arc magmas responsible for the formation of porphyry Cu deposits.

In order to evaluate the effects of magma evolution within crusts of variable thickness on the fertility of arc magmas, petrologic modeling has been used, the details of which are reported in Chiaradia and Caricchi (2017) and Chiaradia (2020b). Such modeling is based on mass balance calculations implemented into the petrogenetic model of hot zone crustal melt generation and evolution, as elaborated by Annen et al. (2006). The rationale of the model is schematically shown in Figure 3. The starting point of the model is the metal endowment (Cu Mt or Au t) of a porphyry deposit. We know that such metal endowment is precipitated from hydrothermal fluids exsolved from a magma (e.g., Gustafson and Hunt, 1975, and subsequent studies). Therefore, the metal endowment is directly tied to the amount of hydrothermal fluid through the metal concentration in it and the precipitation efficiency of the metal from such a fluid.

The metal (Cu, Au) concentration in the fluid is linked to the metal content in the magma, from which such a fluid has exsolved, through the fluid-melt partition coefficient of the specific metal. Such partition coefficient can be variable depending on several parameters (e.g., depth of fluid exsolution, melt composition, fluid composition). All these parameters are difficult to constrain; therefore, a stochastic approach has been chosen in which partition coefficients vary within a range that encompasses the most common geologic situations of porphyry-related fluids (i.e., $D^{Cu}_{fluid-melt}$ = 2–100 and $D^{Au}_{fluid-melt}$ = 10–100; see Chiaradia and Caricchi, 2017 and Chiaradia, 2020b, and references therein). The dependence of the metal concentration in the fluid from the metal concentration in the melt can be tackled by considering again a range of metal contents typical of magmas associated with porphyry deposits (Chiaradia, 2014). For such a purpose the Cu contents of intermediate magmas from thick arcs have been used. Therefore, the model presented here is based on a conservative low Cu content of intermediate magmas from thick arcs (~20–40 ppm). Whereas anomalously high Cu enrichment in magmas may occur (see above) and may further contribute to an increased fertility of the magma, the good agreement between model results and real porphyry Cu data (see below) suggests that such Cu magmatic enrichment is not necessary and probably, looking statistically at recent arc magma data, not widespread.

The amount of hydrothermal fluid that can be exsolved from a magma is more complex to determine. For the sake of simplicity, I have considered that the exsolved fluid is pure H_2O, which is by far the largest constituent of a magmatic arc fluid (e.g., Wallace, 2005). The maximum H_2O content (or solubility) of a magma is a function of two main parameters: pressure and melt composition. H_2O solubility increases with pressure and with increasing SiO_2 content in the melt (e.g., Newman and Lowenstern, 2002; i.e., a rhyolite magma may contain more H_2O in solution than a basalt magma at equal depth). However, to determine the absolute amount of H_2O necessary to precipitate the observed mass of metal in porphyry deposits, we need to also know the amount of magma that contains a specific concentration of H_2O. In order to determine the amount of magma from which the necessary amount of fluid and Cu can be exsolved to precipitate the observed metal content (assuming precipitation efficiencies between 100 and 50%: Figs. 4–7), the magma generation and evolution model of the hot crustal zones of Annen et al. (2006) has been used.

The model (Chiaradia and Caricchi, 2017; Chiaradia, 2020b) starts with basaltic melts generated in the mantle wedge, followed by injection into the crust at a long-term rate typical of average arc magma fluxes (e.g., ~0.001 km^3/yr). Injection occurs as sills at variable crustal depths (between 0.15 and 0.9 GPa, corresponding to ~5- and ~30-km depth: Fig. 4). After injection, the basaltic melt, initially at 1,280°C, starts

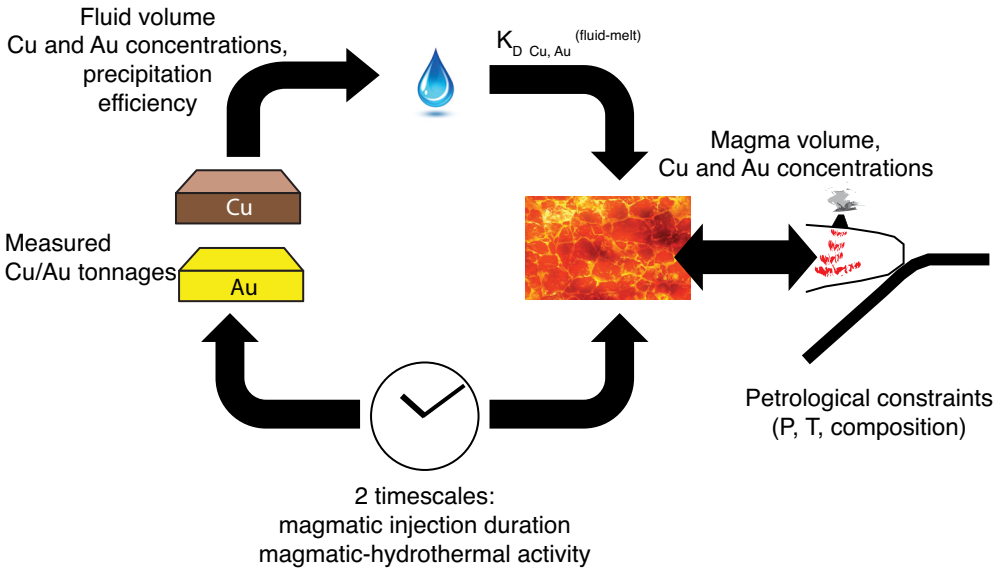

Fig. 3. Conceptual model of the petrologic model used in this study. For explanation see text.

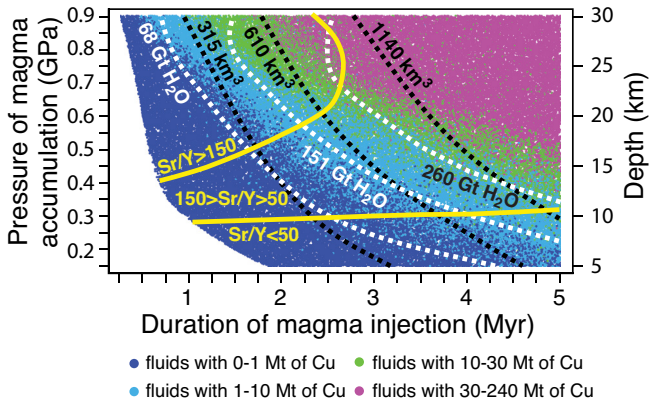

Fig. 4. Results from Monte Carlo simulations for the generation of magmatic systems capable of exsolving fluids with different potential amounts of Cu (100% efficiency of precipitation) in the space of pressure (depth of injection) vs. duration of injection (m.y.). White and black dashed lines indicate the Gt of H_2O dissolved in the hybrid melt and hybrid melt volume in km^3, respectively. Yellow lines represent limits of Sr/Y values of hybrid melts resulting from Monte Carlo simulations (from Chiaradia and Caricchi, 2017). Monte Carlo simulations are from the Excel algorithms attached to Chiaradia and Caricchi (2017) and Chiaradia (2020b).

to cool and crystallize. At the same time, it liberates latent heat of crystallization to the surrounding rocks. Due to continuous injection, the temperature of the host rock increases until a differentiated liquid of the parental basaltic melt will no longer completely crystallize. This will happen when the temperature of the host rocks becomes higher than that of the solidus of the most evolved (felsic) residual melt derived from fractionation of the injected basaltic melt. If the process continues, more magma will accumulate and will progressively shift to less evolved compositions due to the injection of basaltic melt from the mantle. Eventually, host rocks may also start to melt and mix with the residual melt from fractionation of the mantle-derived basalt, producing a hybrid (residual plus crustal) melt.

The hybrid melt grows in volume through time because of the temperature increase of the host crustal rocks induced by the injection of hot basaltic melt. Such growth is larger and faster at deeper crustal levels of injection because of the hotter ambient condition (due to the geothermal gradient), thus requiring less energy for partial melting of the host rocks. In other words, larger amounts of hybrid magma can be produced at deeper crustal levels and after longer injection times, and thus generate the most fertile magmatic systems. This is summarized in Figure 4, where the amounts of Cu and H_2O that can be exsolved, as well as magma volumes, are shown in a depth-of-magma accumulation (pressure) versus duration of magma injection (time) plot. Modeling results show an increasing fertility (i.e., higher amounts of exsolvable Cu) with increasing depth of magma injection and increasing duration of magma injection. Magmatic systems that accumulate at shallow depth (<0.4 GPa, ~13 km), even if for a long time, have lower fertility (<10 Mt exsolvable Cu), since they are always H_2O saturated (Fig. 5) and, therefore, continuously exsolve fluids. The rate of Cu exsolution with such fluids, although capable of generating porphyry Cu deposits with endowments of a few Mt Cu, is too low (even at 100% efficiency) to explain the largest porphyry deposits (>10 Mt Cu; Fig. 6a).

The most fertile magmatic systems are formed at least at depths >~13 km (>0.4 GPa) and preferentially at even greater depths (>20 km, P >0.6 GPa) and during magma injection times >2.5 to 3.0 m.y. (Fig. 4). The reasons for this fertility are associated with the build-up of large crustal magma accumulations that contain high amounts of dissolved H_2O (6–12 wt % H_2O; Fig. 5b). These H_2O concentrations are consistent with water estimates of magmatic systems associated with porphyry Cu deposits (10–12 wt %) using phase equilibria and zircon saturation thermometry (Lu et al., 2015). In other words,

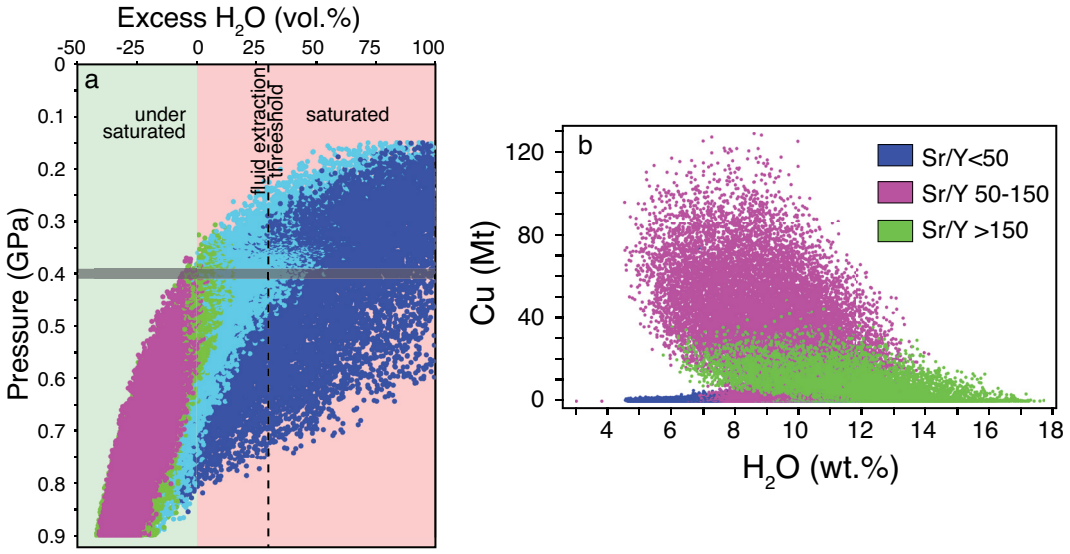

Fig. 5. (a). Pressure vs. excess H_2O (vol %) plot of the Monte Carlo simulations coded for different Cu endowments. The most fertile systems are formed at P >0.4 GPa and are always H_2O undersaturated. (b). Cu (Mt) vs. H_2O (wt %) plot of the Monte Carlo simulation, showing that the most fertile systems correspond to Sr/Y values comprised between 50 and 150. Monte Carlo simulations are from the Excel algorithms attached to Chiaradia and Caricchi (2017) and Chiaradia (2020b). The fluid extraction threshold is from Rintoul and Torquato (1997).

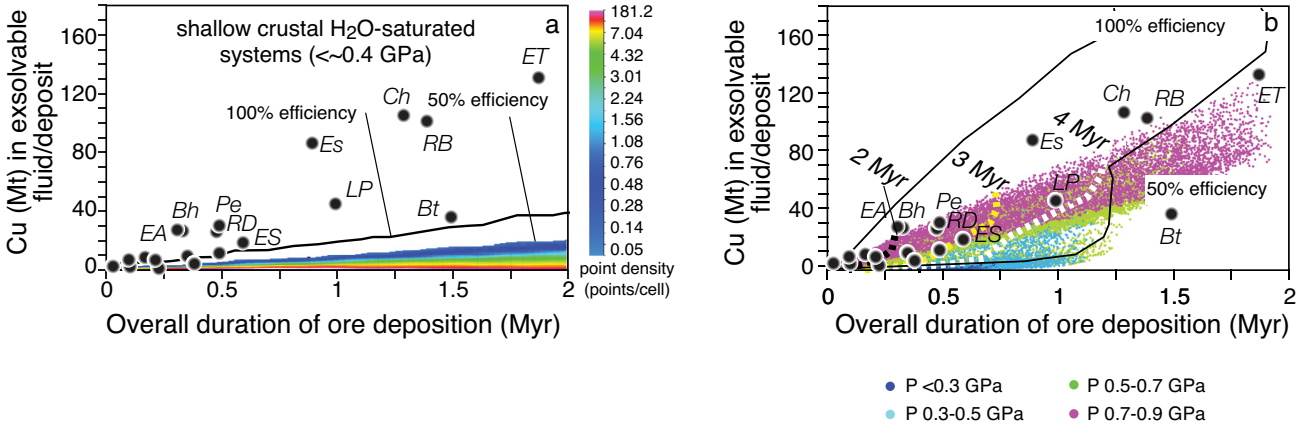

Fig. 6. (a). Monte Carlo simulations of Cu (Mt) in excess fluid (50 and 100% precipitation efficiencies) vs. overall duration of ore formation (m.y.) for H_2O-saturated magmatic systems formed at crustal depths <~0.4 GPa. (b). Cu (Mt) in the exsolvable fluid of hybrid melts (50 and 100% precipitation efficiencies) after injection times of 0 to 5 m.y. vs. the overall duration of the ore deposition (m.y.). Color classes indicate different pressures of magma accumulation. Thick-colored (black, yellow, white) dashed lines represent periods of magma injection at corresponding depths (modified from Chiaradia and Caricchi, 2017). Point density in panel (a) indicates the number of simulations falling within a cell unit of the plotting software (ioGAS). All porphyry deposit data plotted are freely available as a Supplementary Excel table attached to Chiaradia (2020b). Monte Carlo simulations are from the Excel algorithms attached to Chiaradia and Caricchi (2017) and Chiaradia (2020b). Abbreviations: ET = El Teniente, Ch = Chuquicamata, RB = Rio Blanco, Bt = Butte, Es = Escondida, LP = Los Pelambres, Pe = Pebble, RD = Reko Diq, ES = El Salvador, Bh = Bingham, EA = El Abra.

these magmatic systems are large and H_2O-rich because they accumulate at deep crustal levels, which favors both the formation of large magma accumulations (because of favorable thermal conditions) and increased H_2O solubility (because of high pressure). The large magma and fluid volumes compensate for the low Cu contents of intermediate arc magmas in thick crusts (~20–40 ppm) and are capable of exsolving (at 100% efficiency) up to 240 Mt Cu (Fig. 4). The magma volumes of these systems are >1,000 km^3, which allow them to contain >260 Gt of dissolved H_2O (Fig. 4). The Sr/Y values obtained from the intracrustal petrologic modeling above (Chiaradia and Caricchi, 2017) range from 50 to 150 for the most fertile magmatic systems (Figs. 4, 5), which is the same range observed for known Cu-rich porphyry Cu-Au deposits (Loucks, 2014). Therefore, according to the model presented here, the association of Cu-rich porphyry Cu-Au deposits with intrusions that have Sr/Y values of 50 to 150 (so-called adakite-like values; Richards and Kerrich, 2007) is the result of such magmatic systems being formed at depths (>~20 km) and during periods of injection (>2.5–3.0 m.y.), which are the most favorable to accumulate the largest amounts of magma, H_2O, and Cu. The multimillion year premineralization magmatic history, with a steady increase of Sr/Y values through time for several porphyry-type deposits (e.g., Los Pelambres, Reich et al., 2003; Yanacocha, Chiaradia et al., 2009; El Teniente, Stern et al., 2010; El Abra, Rabbia et al., 2017), is consistent with this model.

Large accumulations of magma at deep (>~20 km) crustal levels, as required by the model for fertile magmas, are favored by thick crust and a compressional regime in the overriding plate. Such combination slows the ascent of magma and favors its accumulation at deep levels (e.g., Takada, 1994; Tosdal and Richards, 2001; Cembrano and Lara, 2009) to develop large and H_2O-rich magmatic systems (Fig. 5) at pressures sufficient to prevent H_2O saturation, with a typically high Sr/Y signature (Figs. 4, 5). This agrees with the observation that porphyry Cu formation is preceded by long periods of compression in the geologic record (Sillitoe, 2010, and references therein).

Petrologic simulations indicate that fertile magmatic systems accumulated at P >0.4 and up to 0.9 GPa, despite being H_2O-rich (6–12 wt % H_2O), are H_2O undersaturated (Fig. 5). In this way they can accumulate large amounts of H_2O and Cu within a magma reservoir that grows larger with time without exsolving fluid and metals. In order to exsolve fluids and form porphyry deposits, the fractionated magmas need to rise to shallower crustal levels. Simulations indicate that such fertile magmas, assuming no crystallization during ascent, will become H_2O saturated at pressures of 0.25 to 0.55 GPa (~8- to 18-km depth; Chiaradia and Caricchi, 2017). Such depths are consistent with geophysical, petrologic, and mineral barometric data for the parental magma reservoirs that feed the porphyry apophyses associated directly with the ore shells at ~1- to 5-km depth (e.g., Sillitoe, 2010, and references therein; Murakami et al., 2010).

The ascent of magmas from the deep accumulation zone to the shallower crustal levels of emplacement of the parental magma reservoir is likely promoted by a change in the tectonic regime of the overriding plate, from compression to a regime more favorable to shallow intrusion (e.g., Tosdal and Richards, 2001). This is consistent with the observation that porphyry Cu deposits are formed at the transition between a variably long period of compression and a near-neutral stress regime (Tosdal and Richards, 2001; Bertrand et al., 2014). Topographic anomalies on the subducting plate (e.g., aseismic ridges and plateaus) or major plate reorganization (e.g., changes in plate direction, subduction speed, slab dip) could ultimately be responsible for the changes in the tectonic regime of the overriding plate with consequences for magmatism and mineralization (e.g., Cooke et al., 2005; Rosenbaum et al., 2005; Chiaradia et al., 2009). During this period

of tectonic relaxation, the large accumulations of magma may ascend from the deep crustal reservoir and incrementally build-up the parental magma chamber that feeds even shallower porphyry apophyses directly associated with the ore. The timescales of the transfer of the magma accumulations from the deep crustal zone influences the overall duration of the magmatic-hydrothermal mineralizing events. The average rate of Cu precipitation predicted by the petrologic simulations (Fig. 6b) is consistent with that observed in natural porphyry systems (for precipitation efficiencies ≥50 and <100%), if sufficient magma, H_2O, and Cu have been previously accumulated in the deep crustal zone (which depends on the duration of the injection interval; Fig. 6b).

Available geochronological data coupled with Cu endowments of porphyry deposits suggest that there is a relationship between the overall duration of the mineralizing process and Cu tonnage (Fig. 6b). This is consistent with the episodic and pulsed transfer of magma plus its fluid and Cu content from the deep crustal reservoir to shallower depths, where porphyry mineralization ultimately occurs. Such episodic and incremental injection of porphyry intrusions and associated hydrothermal activity is indicated by crosscutting field relationships (e.g., Sillitoe, 2010) and their geochronologic dating (e.g., von Quadt et al., 2011; Li et al., 2017). The model discussed here suggests that the greater the number of episodic magma intrusions into the shallow parental magma chamber (~8- to 18-km depth), the larger the overall size of the deposits, resulting from the incremental build-up of short-lived magmatic-hydrothermal pulses of porphyry mineralization injected from the parental magma chamber (cf. Mercer et al., 2015). Factors that control the number and overall duration of magmatic pulses from the deep reservoir (where the magmas attain their Cu endowment) are the availability of magma in the deep reservoir and the tectonic regime. The former limits the amount of magma that can be transferred to shallower levels (Chiaradia and Caricchi, 2017). The latter may shut off the magma transfer if there is a transition from a transfer-favorable near-neutral stress regime to a compressional regime that is unfavorable for magma transfer or to an excessively extensional regime that favors eruption (e.g., Tosdal and Richards, 2001).

The amount of available magma in the deep reservoir should be proportional to the premineralization timescales of magma accumulation (Fig. 6b). Such timescales can be inferred from the geochronology of premineralization magmatic events in the porphyry district. There are insufficient geochronologic data on such timescales, but those available indicate that similarly long (several m.y.) precursor magmatic activity occurs for porphyry deposits with large differences in Cu endowments (El Teniente 130 Mt Cu, Stern et al., 2010; Los Pelambres 46 Mt Cu, Reich et al., 2003; El Abra 8.8 Mt Cu, Rabbia et al., 2017). This may suggest that magma availability, although essential for a high fertility of the magmatic system (Fig. 6b), is not always the only necessary factor determining the size of a Cu deposit. Changes in tectonic regime could have an important influence on the Cu endowment of porphyry deposits (Tosdal and Richards, 2001; Bertrand et al., 2014; Richards, 2018) by interrupting the transfer of magma from a large and potentially fertile deep reservoir to the shallower level where mineralization occurs.

Model validation tests

The model presented above can be tested for the parameters for which data are available, such as Cu endowments, Sr/Y values of magmatic rocks, and overall duration of the mineralizing process. Limited data are available for La/Yb and duration of precursor magmatic activity, so these parameters have a limited use in a validation test.

Figure 7 shows the distribution of porphyry deposits with the model simulations in Cu tonnage versus Sr/Y of magmatic rocks (Fig. 7a-b), and overall duration of mineralizing event versus Cu tonnage (Fig. 7c). In both cases there is a good agreement between model simulations and actual porphyry data. Nearly all porphyry Cu deposits fall in the 50 to 150 range of Sr/Y values of their associated magmatic rocks (Fig. 7a). Modeling also indicates a similar distribution, suggesting that the modeled magmatic systems associated with the largest porphyry Cu deposits have Sr/Y values of 50 to 150, and that modeled deposit size decreases both for lower and higher Sr/Y values of the associated magmatic systems. This translates into similar frequency distribution plots of actual porphyry Cu deposits and simulations that indicate a low probability to form porphyry deposits with >20 Mt Cu where Sr/Y values are <50 and >150 (Fig. 7b).

In the Sr/Y range 50 to 150, where most porphyry systems plot, the sizes of the deposits vary widely. The smaller deposits are those with the higher probabilities to form both in the real world and in the simulations (Fig. 7b). The main control on this variation (Fig. 7c) is likely the overall duration of the mineralizing process, as discussed previously. A higher number of short-lived individual magmatic-hydrothermal pulses, spaced in time, should result in a longer timescale of the entire mineralizing process and, therefore, should also result in an overall larger Cu endowment, assuming that every pulse contributes to an incremental addition of Cu metal. There is a good agreement between predicted and modeled Cu endowments (Fig. 7c; see the match of colors corresponding to Cu endowments between porphyry deposits and Monte Carlo simulations). Exceptions are Grasberg, Bingham, and Reko Diq, which fall in a field of lower modeled Cu endowments with respect to the real endowments of these deposits (Fig. 7c). This might suggest that additional controls on the endowments of these deposits are at play, such as higher magmatic Cu contents in alkaline magmas (Grasberg and Bingham?, see also Keith et al., 1997; Core et al., 2006) or a higher precipitation efficiency (Reko Diq?). Clearly more work is needed to understand the systematics controlling metal endowments in porphyry Cu-Au deposits.

What role for H_2O-rich primary basalts in porphyry Cu deposit endowments?

As discussed above, H_2O is of critical importance in determining the fertility of magmas to form porphyry Cu deposits (see also Chiaradia, 2020a; Rezeau and Jagoutz, 2020). The difference in H_2O content between primary arc basalts and MORBs has been highlighted above as a first-order control in the fertility of arc magmas. On the other hand, primary arc magmas may have somewhat variable H_2O contents (2–6 wt %; Plank et al., 2013) and it has been suggested that anomalously H_2O-rich primary basalts, resulting from dehydration of large-scale

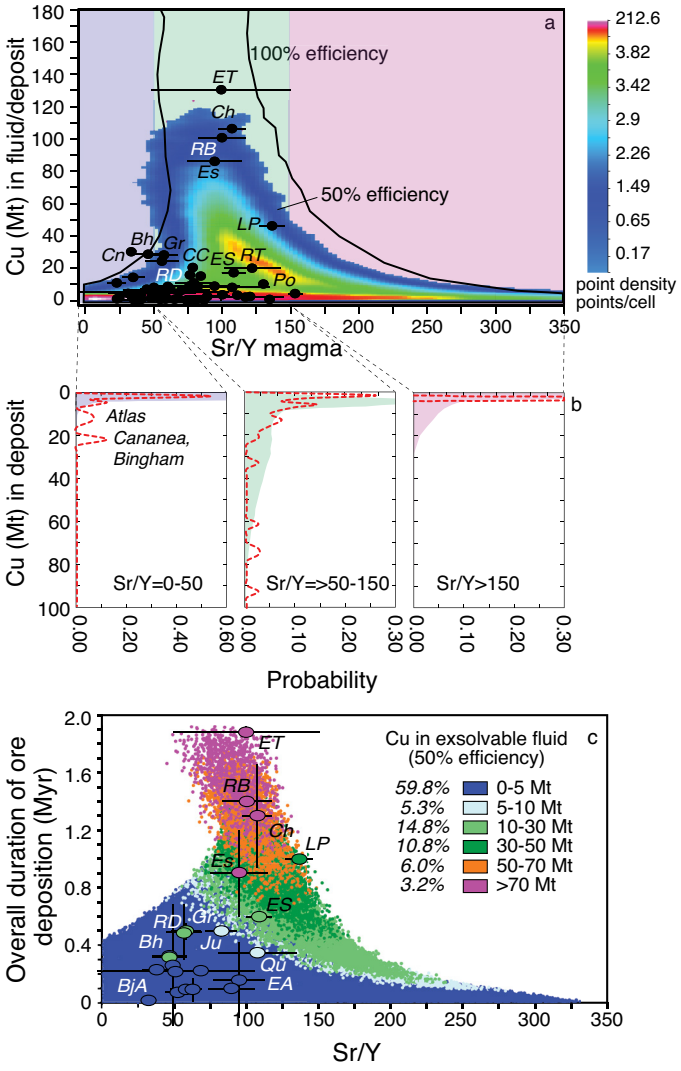

Fig. 7. (a). Cu (Mt) in fluid exsolvable (50 and 100% precipitation efficiencies) from magmatic systems formed at various depths (~5–30 km) and after different injection times (0–5 m.y.) vs. modeled hybrid melt Sr/Y values. Also reported are the Cu endowments and average Sr/Y values (±1σ) of porphyry Cu deposits for which data are available (see Supplementary Excel table attached to Chiaradia, 2020b). (b). Probability distribution of modeled magmatic system productivity (50% precipitation efficiency) for the three intervals of Sr/Y values determined by the average ±1σ (100 ± 50) values of natural porphyry Cu deposits (i.e., <50, 50–150, >150). The red dashed lines show the probability distributions for natural porphyry deposits. (c). Overall duration of the ore deposition (m.y.) vs. Sr/Y values plot of the Monte Carlo simulations color-coded for modeled exsolvable Cu at 50% precipitation efficiency. Also shown are porphyry Cu deposits for which duration of mineralization and Sr/Y data of associated magmatic rocks are available (see Supplementary Excel table attached to Chiaradia, 2020b). Monte Carlo simulations are from the Excel algorithms attached to Chiaradia and Caricchi (2017) and Chiaradia (2020b). Abbreviations: Bh = Bingham, CC = Cerro Colorado, Ch = Chuquicamata, Cn = Cananea, Es = Escondida, ES = El Salvador, ET = El Teniente, LP = Los Pelambres, Po =Potrerillos RB = Rio Blanco, RD = Reko Diq, RT = Radomiro Tomic.

fracture zones of the subducting oceanic slab, could be more fertile and associated with larger porphyry deposits (e.g., Rosenbaum et al., 2005; Richards and Holm, 2013). These fracture zones are more intensely serpentinized than normal oceanic crust and could liberate more H_2O during the subduction process.

However, petrologic modeling shows that the maximum fertility of derivative intermediate-felsic magmas is for parental basalts with H_2O contents between 2 and 6 wt % (Chiaradia, 2020a); for lower and higher H_2O contents in the parental basalt, fertility decreases. Whereas the decrease in fertility for low H_2O contents in primary basalts is understandable (see also Chiaradia, 2020a; Rezeau and Jagoutz, 2020) and, at its extreme, is the reason why MORBs (having H_2O contents of ~0.25 wt %; Wallace, 2005) cannot form economic porphyry deposits, the decrease of fertility with increasing H_2O contents is counterintuitive. The reason is that excessively H_2O-rich primary basalts become H_2O-saturated at deep crustal levels, thus losing a significant amount of H_2O and especially Cu at those depths (Chiaradia, 2020a). When they rise to shallower crustal levels, where they can form porphyry deposits, such magmatic systems are significantly more depleted in H_2O and especially Cu than magmatic systems associated with the evolution of parental basalts having 2- to 6-wt % H_2O (Chiaradia, 2020a). Additionally, H_2O-rich magmas, exsolving H_2O at deep crustal levels, are more likely to crystallize and freeze there. This prevents them from ascending to shallow crustal levels from where only they could form porphyry deposits.

The 2- to 6-wt % range of H_2O content in the most fertile primary basalts, as indicated by petrologic modeling, coincides with the range (2–6 wt %) and average measured H_2O content of basaltic arc melts (3.9 ± 0.4 wt %; Plank et al., 2013). This suggests that arc magmas with normal H_2O contents, and also standard S, Cl, and Cu contents, are potentially all equally fertile (see also Cline and Bodnar, 1991; Chelle-Michou et al., 2017); thus, other processes control their fertility in the arc environment, the most important of which are volumes of magmas and of associated fluids.

Cu-Rich Versus Au-Rich Porphyry Cu-Au Deposits

The above model has been applied to Cu endowments of porphyry Cu-Au deposits. However, porphyry Cu-Au deposits can also contain significant amounts of gold (e.g., Sillitoe, 2000). Indeed, porphyry Cu-Au deposits define distinct linear arrays in terms of Cu versus Au endowments, and also the overall duration of mineralization process versus Au endowment (Fig. 8; Chiaradia, 2020b). This allows the definition of Cu-rich porphyry Cu-Au deposits (Au/Cu ~4 × 10^{-6}) and Au-rich (Au/Cu ~80 × 10^{-6}) porphyry Cu-Au deposits (see above and Fig. 8a). From available geochronologic data the maximum duration of Au-rich porphyry Cu-Au deposit formation is shorter (<~0.5 m.y.) than that of Cu-rich porphyry Cu-Au deposits (<~2 m.y.), which results in average rates of gold deposition that are much higher in Au-rich porphyry Cu-Au deposits (~4,500 t Au/m.y.) than in Cu-rich porphyry Cu-Au deposits (~100 t Au/m.y.; Fig. 8b).

All Cu-rich porphyry Cu-Au deposits are associated exclusively with typical calc-alkaline magmas in synsubduction, Andean-type porphyry settings (Fig. 8). In contrast, Au-rich porphyry Cu-Au deposits are associated not only with calc-alkaline synsubduction magmas but also with high-K calc-alkaline and alkaline magmas in postsubduction settings, including postcollisional to extensional tectonic regimes (Fig. 8; Chiaradia, 2020b).

Chiaradia (2020b) attributed the existence of these two distinct trends to different precipitation efficiencies of gold at

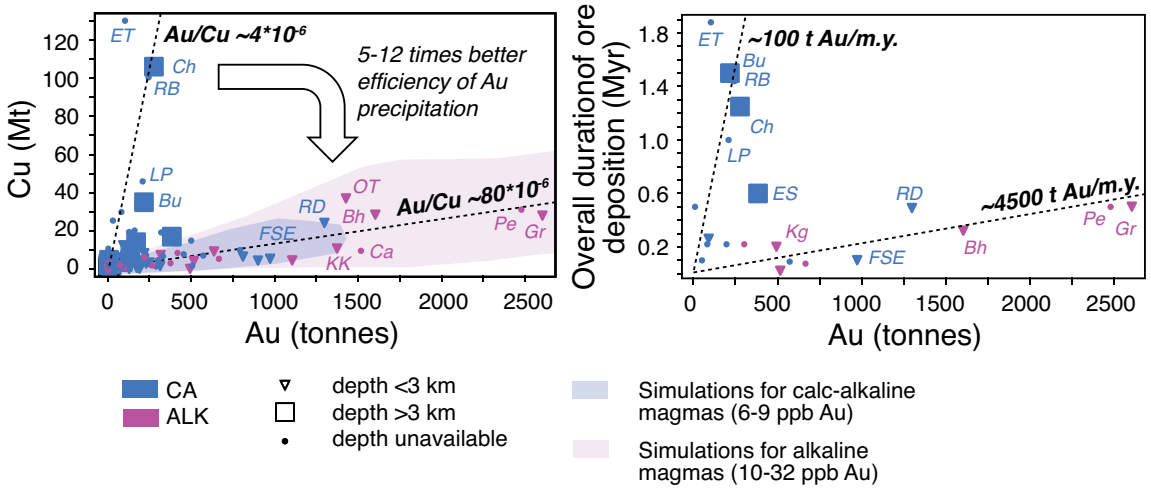

Fig. 8. (a) Cu (Mt) vs. Au (t) of porphyry Cu-Au deposits. (b). Ore duration (m.y.) vs. Au (t) of porphyry Cu-Au deposits. All deposits are roughly distributed along either one or the other of the two dashed lines allowing the identification of two distinct families of porphyry Cu-Au deposits, the Cu-rich (Au/Cu ~4 × 10^{-6} and ~100 t Au/m.y.) and the Au-rich (Au/Cu ~80 × 10^{-6} and ~4,500 t Au/m.y.). The dashed lines represent average rates of Cu and Au deposition and are not statistically best-fitted lines. The pale-pink field represents Monte Carlo simulations carried out for Au precipitation efficiencies that are ~5 times higher for the alkaline system-related Au-rich trend than for the calc-alkaline system-related Cu-rich trend. The pale-blue field represents simulations carried out for Au precipitation efficiencies that are ~12 times higher for the calc-alkaline system-related Au-rich trend than for the calc-alkaline system-related Cu-rich trend. The Au concentrations used for modeling are from Moss et al. (2001) for calc-alkaline magmas and from Rock and Groves (1988) for alkaline magmas. All porphyry deposit data plotted are freely available as a Supplementary Excel table attached to Chiaradia (2020b). Abbreviations: Bh = Bingham, Bu = Butte, Ca = Cadia, Ch = Chuquicamata, ES = El Salvador, ET = El Teniente, Gr = Grasberg, Kg = Kisladag, Kk = Kalmakyr, LP = Los Pelambres, OT = Oyu Tolgoi, RB = Rio Blanco, RD = Reko Diq.

the depths of formation of Cu- and Au-rich porphyry Cu-Au deposits (see also Fig. 8). Murakami et al. (2010) showed that Au/Cu ratios correlate systematically with the depth of porphyry formation, with shallower depth corresponding to higher Au/Cu values and vice versa. These authors attributed this major variation in the gold grade with depth to the transport of Cu and Au in an S-rich fluid phase. At shallow depths (<~3 km), Au and Cu coprecipitate due to the rapid decrease in density of the fluid. In contrast, at greater depths, Cu precipitates due to rapid fluid cooling, whereas Au remains in solution in the ascending fluid.

With the currently available quantitative data on the depth of formation of porphyry deposits, the largest Au-rich porphyry Cu-Au deposits form at shallow depths (<~3 km; Fig. 9), irrespective of their petrogenetic association with calc-alkaline or variably alkaline magmas. In contrast, the largest Cu-rich porphyry Cu-Au deposits form at deeper levels (>~3 km). More quantitative data on depth of formation of porphyry Cu-Au deposits are needed to see whether the correlation between depth and Au/Cu ratios still holds with a broader dataset, including also some of the largest Cu-rich porphyry Cu-Au deposits (e.g., El Teniente, Rio Blanco) that are currently missing (Fig. 8).

Notwithstanding these arguments, not all shallow-formed porphyry Cu-Au deposits are Au rich, nor are all deep deposits large Cu-rich deposits. One reason for this is that a critical factor that determines the size of the deposits is the overall timescale of the mineralizing process, not only for Cu, as discussed previously (Fig. 6b), but also for Au (Fig. 8b).

An important consideration stemming from the petrologic simulations is that the largest Au endowments of the Au-rich porphyry Cu-Au deposits (>~1,300 t Au) can only be explained by a higher Au content in the associated magmas (Fig. 8a; Chiaradia, 2020b). Simulations carried out for calc-alkaline magmas with their average Au contents (Chiaradia, 2020b) are not able to reach the very high Au endowments of the alkaline-related Au-rich porphyry Cu-Au deposits (Fig. 8a). This is consistent with the association of the six largest Au-rich porphyry Cu deposits with variably alkaline magmas (Fig. 8a). Alkaline magmas are known to contain on average higher Au contents than calc-alkaline magmas (Rock and Groves, 1988; see also Fig. 8). In addition, gold is enriched in differentiated alkaline magmas because alkali metals increase sulfur solubility and decrease the partition coefficient of Au between silicate melt and magmatic sulfides (Li et al., 2019).

Distinct Tectonic and Geodynamic Settings for Au- and Cu-Rich Porphyry Deposits?

A remarkable observation using available data is that the depth of formation of porphyry deposits correlates with the average Sr/Y composition of the associated magmatic rocks (Fig. 9), although, as discussed above for the correlations between depth of porphyry formation and Au/Cu ratios, this correlation also needs to be tested by the acquisition of data from more porphyry deposits. For the time being, such a correlation is worth investigation because it concerns two parameters that are measured in completely independent ways. The Sr/Y values are known to be a proxy for the average depth of magma evolution, which broadly correlates with crustal thickness (Chiaradia, 2015). Therefore, such a correlation indicates that when magmas evolve at average deeper levels (higher Sr/Y values), the associated porphyry deposits also form at

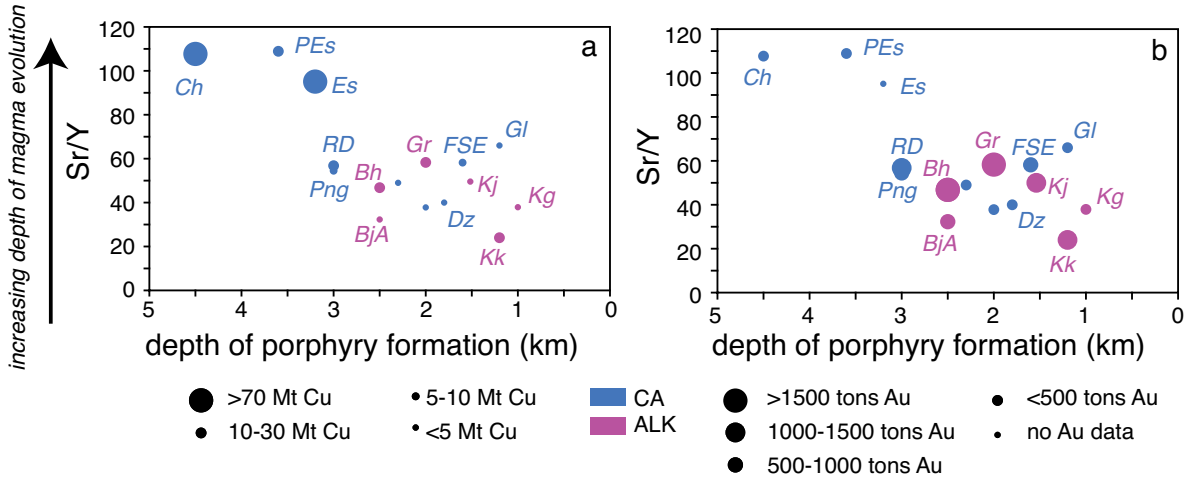

Fig. 9. Depth of formation vs. Sr/Y average values of associated magmatic rocks. The size of the symbols corresponds to different copper (a) and gold (b) tonnages as indicated in the legend. Blue and pink colors of the symbols refer respectively to calc-alkaline and high-K calc-alkaline to alkaline magmatic systems. All porphyry deposit data plotted are freely available as a Supplementary Excel table attached to Chiaradia (2020b). Abbreviations: Bh = Bingham, BjA = Bajo de la Alumbrera, Ch = Chuquicamata, Es = Escondida, FSE = Far South East-Lepanto, Gl = Granisle, Gr = Grasberg, Kg = Kisladag, Kj = Kadjaran, Kk = Kalmakyr, PEs = Pampa Escondida, Png = Panguna, RD = Reko Diq.

deeper levels. In contrast, where magmas evolve at average shallower levels, the associated porphyry deposits form at shallower levels. This suggests that there may be a tectonic and geodynamic control on the formation of Cu- and Au-rich porphyry deposits, as discussed below.

Cu-rich porphyry Cu-Au deposits form preferentially in synsubduction, Andean-type settings, in thick crust of the overriding plate (Fig. 10a). Such deposits require large magma volumes to form, which are accumulated in the lower crust during a long-lasting compressional period. The typical geochemical signature of magmas associated with these deposits is a high Sr/Y composition (100 ± 50), which, together with other geochemical markers (high La/Yb, V/Sc; Loucks, 2014), is an indication of a deep crustal magmatic evolution that is only possible in a thick crust. Subsequent transfer of magma batches from the deep reservoir to a shallower one (Fig. 10b) is necessary to form porphyry Cu mineralization, as discussed above.

In contrast, Au-rich porphyry Cu-Au deposits form at overall shallower levels in association with calc-alkaline magmas, in both thin and thick arc settings, and also in association with variably alkaline magmas in postsubduction to extensional settings (Fig. 10c-d). The lower Sr/Y values of Au-rich porphyry Cu-Au deposits (Fig. 9) suggest that, despite the variety of environments in which they form and the variety of magmatic compositions with which they are associated, the common point is an overall shallower level of magma evolution. This can be the result of formation of these deposits in a thinner crust (island arcs of the SW Pacific), and/or in extensional settings whereby magmas can ascend from the mantle to shallower crustal levels, even where the crust is variably thick (Fig. 10d-e).

Conclusions and Remaining Questions

Porphyry Cu-Au deposits are a major source of copper and a significant source of gold to our society. Understanding how these deposits form and why they have variable metal endowments is essential for their exploration. This overview has addressed some of the magmatic controls on the formation of these deposits. The association of porphyry Cu-Au deposits with syn- and postsubduction settings suggests that source processes, unique to the convergent margins, exert a primary control on the formation of these deposits. By comparison with MORBs, convergent-margin primary arc basalts are clearly enriched in H_2O, Cl, and S, perhaps Au but not in Cu. H_2O, Cl, and S are all essential ingredients to form porphyry deposits and this may explain why they are indirectly associated uniquely with primary basaltic melts derived from a slab-metasomatized mantle, either synchronously with porphyry formation (synsubduction porphyry deposits) or prior to porphyry formation (postsubduction porphyry deposits).

However, porphyry deposits are directly associated with intermediate to felsic magmas derived from these primary basalts and are not found in primitive arc magmas developed in thin oceanic crust (e.g., Mariana, Kermadec), despite the knowledge that primary basalts in these arcs contain comparable contents of H_2O, S, and Cl to those of thicker arcs where porphyry deposits form. This suggests that intracrustal magmatic evolutionary processes play a prominent role in determining the fertility of arc magmas.

In particular, mass balance calculations combined with petrologic modeling of intracrustal magmatic evolution indicate that metal endowments of porphyry Cu-Au deposits depend on the volume of magma associated with the porphyry deposit, the depth at which such volume is accumulated (which also controls the amount of dissolved H_2O in the magma), and the duration of the magmatic-hydrothermal mineralization event. Magma volumes grow larger at greater depths in the crust, simply because of energetic constraints. The duration of the magmatic-hydrothermal mineralization depends on the transfer of magma from the deeper accumulation zone to shallower crustal levels where fluid exsolution occurs. The average duration of such transfer seems to ultimately control the size of the deposits through an

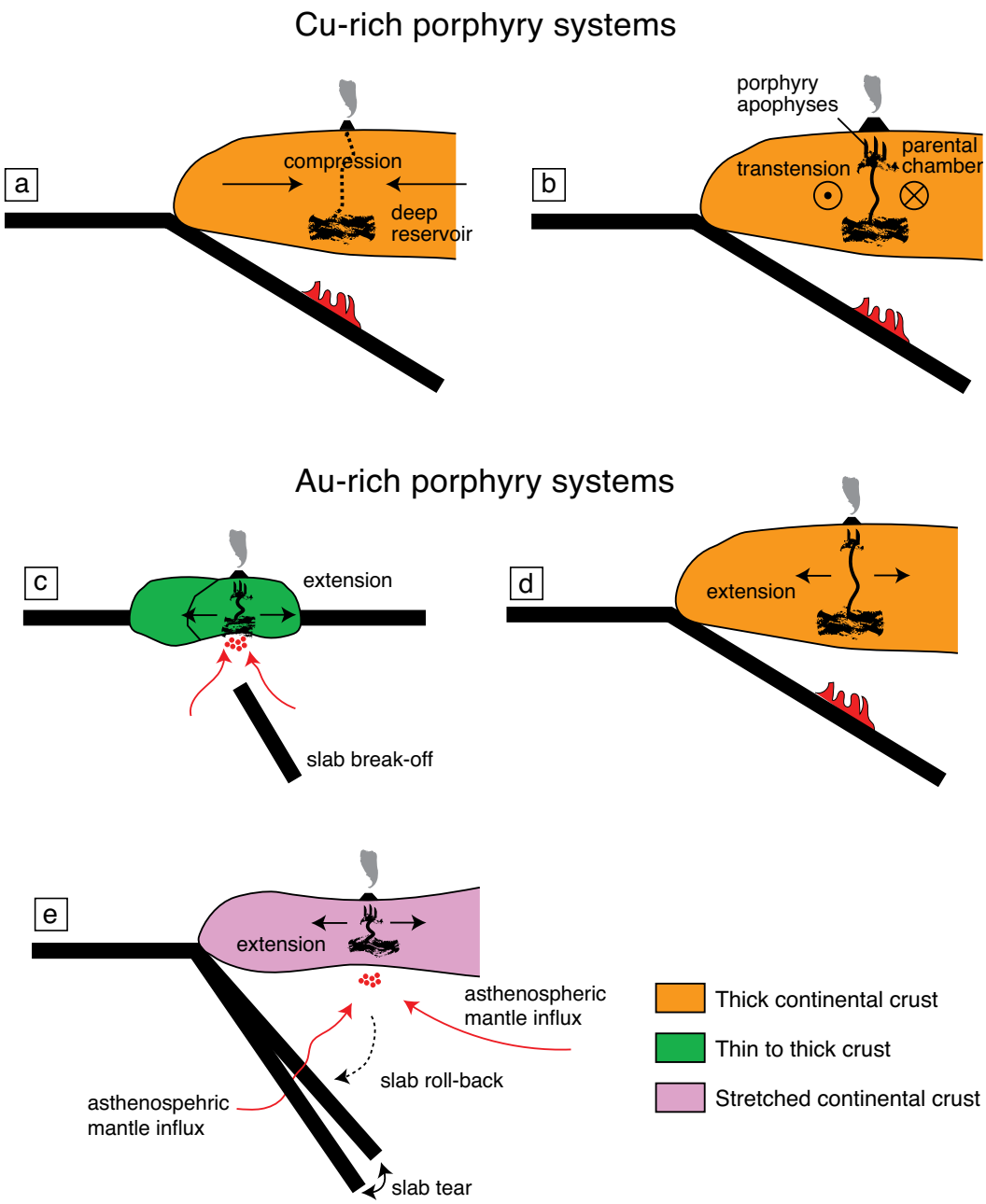

Fig. 10. Sketches of the geodynamic environments of Cu-rich (a)-(b) and Au-rich porphyry Cu-Au deposits (c)-(e). Cu-rich porphyry Cu-Au deposits form in synsubduction thick continental arcs. They are preceded by a long-lived (several m.y.) magmatic accumulations at deep crustal levels, that are favored by overall long-lasting compression (a). Eventually, a change in the stress within the overriding plate leading to near-neutral horizontal stress or transtension allows magmas to rise from the deep accumulation zones to shallower levels where porphyry deposits form (b). Au-rich porphyry Cu-Au deposits may form in more varied and complex geodynamic settings: postsubduction extension in thin or thick arcs (e.g., Grasberg, Batu Hijau, Kisladag); (c). Synsubduction episodic extension in thick arcs (e.g., Maricunga belt); (d). Synsubduction extension in intermediate thick arcs (e.g., Bingham, Kalmakyr?); (e). Au-rich porphyry Cu-Au deposits are commonly associated with variably alkaline magmas especially in settings (c) and (e).

episodic accumulation of metals associated with short-lived magmatic-hydrothermal pulses. However, more detailed geochronologic dating of multiple magmatic-hydrothermal pulses (especially on young, i.e., <10 Ma, deposits for which geochronologic resolution is optimal; Chiaradia et al., 2013) should be conducted in order to determine how, during the overall duration of the mineralizing event, metal precipitation occurs (e.g., several events with similar magnitudes of metal precipitation, or an irregular distribution of the metal precipitation within the overall duration of the mineralizing event, or other configurations?). Such determinations will assist the understanding of how porphyry Cu-Au deposits form, and how they are associated with the processes of intracrustal magma evolution at greater depth.

Porphyry Cu-Au deposits show a distinct metal endowment distribution, forming either a Cu- or Au-rich trend. Such trends are associated with somewhat distinct geochemical signatures of magmas, in particular a higher Sr/Y average composition of magmas associated with Cu-rich porphyry deposits (Sr/Y ~100 ± 50) than those associated with Au-rich porphyry Cu-Au deposits (Sr/Y ~50 ± 25). Such differences in the Cu versus Au endowments of porphyry deposits could ultimately be attributed to their formation in distinct tectonic and geodynamic settings. Copper-rich porphyry Cu-Au deposits form in magmatic arc systems developed within a thick overriding plate and are preceded by a long-lived magmatic accumulation at deep crustal levels under a broadly compressional regime. Such magmas are subsequently transferred to and intruded at shallower levels, probably during a switch from compression to near-neutral stress conditions. The continuous intrusion of magma batches from the deep accumulation zone to the shallow crust leads to episodic magmatic-hydrothermal events that might incrementally construct variably sized porphyry Cu deposits. Under these conditions the correlation between higher average Sr/Y values of magmas and greater depths of formation of Cu-rich porphyry Cu-Au deposits suggests that average magma evolution at deeper crustal levels is also accompanied by porphyry emplacement at deeper levels. The latter favors a decoupling between Cu and Au endowments, perhaps due to Cu precipitating at deep levels due to rapid cooling of the exsolved fluid and Au remaining in solution and ascending to shallower levels.

Gold-rich porphyry Cu-Au deposits form in thin arcs (e.g., the island arcs of the SW Pacific) and/or in thick arcs during syn- to postsubduction extensional periods that allow an overall shallower evolution of magmas. Under these conditions, porphyry deposits seem also to be formed at shallower levels, where Cu and Au are coprecipitated. In other words, at these shallower levels the precipitation efficiency of gold compared to Cu is increased with respect to Cu-rich systems. The six largest Au-rich porphyry Cu-Au deposits are all associated with variably alkaline rocks, suggesting a petrogenetic control on their exceptionally Au-rich nature (see also Jensen and Barton, 2000; Sillitoe, 2000), which is supported by petrologic modeling (Chiaradia, 2020b). Such alkaline magmas are typically associated with postsubduction extensional geodynamic settings, in which a variety of Au-rich deposits (including epithermal) form.

Because of the overall shallower evolution of the magmatic systems associated with Au-rich porphyry Cu-Au deposits, the latter cannot be associated with the very large magma accumulations that are required to feed the largest Cu-rich porphyry deposits. This is again due to energetic constraints that make it difficult to build up large magma accumulations by melt injection at shallow crustal levels. This is also supported by the overall shorter durations of the mineralizing process in Au- rather than in Cu-rich porphyry Cu-Au deposits. Nonetheless, such reasoning is based on the assumption that in the postsubduction, extensional setting of Au-rich porphyry Cu-Au deposits, average magma fluxes are similar to synsubduction setting. Investigations attempting to determine the magmatic fluxes in this setting would be necessary to better constrain such a model.

Because the shallower Au-rich systems are not associated with extremely large magma accumulations at depth, and form during shorter mineralization timescales, they cannot reach the Cu endowments of the largest Cu-rich deposits, although several of them contain quite high Cu endowments (e.g., Grasberg, Bingham). Also, in the case of Au-rich porphyry Cu-Au deposits, the endowments of both Au and Cu appear to be controlled by the overall duration of the mineralizing event. The difference is that in this environment, mineralization timescales are shorter than ~0.5 m.y., whereas Au precipitation rates are higher, ultimately resulting in the high Au/Cu trends typical of Au-rich porphyry Cu-Au deposits.

The positive correlation between average depth of magma evolution (Sr/Y ratios) and porphyry emplacement is somewhat puzzling. Whereas average magma evolution at shallow depths must necessarily result in porphyry emplacement at even shallower depths, it is not clear why magmatic evolution at greater depths should result in porphyry emplacement also at deeper levels (Fig. 9). Whether this is controlled by tectonics or by self-constrained parameters of the magmatic system (e.g., rheology, composition, thermal maturation of the crust) needs to be investigated in more detail.

Acknowledgments

I take this opportunity to wholeheartedly remember Jeremy Richards for the great human and scientific heritage he left to the world of economic geologists. I first met Jeremy at a UNESCO-SEG-SGA course in Quito, 2003, and we immediately started speaking about "adakites" and their role in the formation of porphyry deposits. Without his works, which have been a constant source of inspiration for me, I could not have written this overview. Thanks Jeremy! I would also thank Simon Large, Yongjun Lu, and Jeff Hedenquist for their reviews that contributed to improve a previous version of this work, as well as Rui Wang and Ali Sholeh for inviting me to contribute to this Special Publication. This overview is based on several years of research and is also the result of data collected by and discussions carried out with numerous Ph.D. and M.Sc. students, as well as with colleagues in Switzerland and around the world. Research results discussed in this review were obtained through several grants of the Swiss National Science Foundation (N. 200021-109626, 200020-117616, 200020_126896, 200020_137663, 200020_149147, 200020_162415, 200021_169032).

REFERENCES

Aiuppa, A., Baker, D.R., and Webster, J.D., 2009, Halogens in volcanic systems: Chemical Geology, 263, p. 1–18.

Alonso-Perez, R., Müntener, O., and Ulmer, P., 2009, Igneous garnet and amphibole fractionation in the roots of island arcs: Experimental constraints on H_2O undersaturated andesitic liquids: Contributions to Mineralogy and Petrology, v. 157, p. 541–558.

Annen, C., Blundy, J.D., and Sparks, R.S.J., 2006, The genesis of intermediate and silicic magmas in deep crustal hot zones: Journal of Petrology, v. 47, p. 505–539.

Audétat, A., and Simon, A.C., 2012, Magmatic controls on porphyry copper genesis: Society of Economic Geologists Special Publication 16, p. 553–572.

Bénard, A., Klimm, K., Woodland, A.B., Arculus, R.J., Wilke, M., Botcharnikov, R.E., Shimizu, N., Nebel, O., Rivard, C., and Ionov, D.A., 2018, Oxidising agents in sub-arc mantle melts link slab devolatilisation and arc magmas: Nature Communications, v. 9, p. 1–10, no. 3500.

Bertrand, G., Guillou-Frottier, L., and Loiselet, C., 2014, Distribution of porphyry copper deposits along the western Tethyan and Andean subduction

zones: Insights from a paleotectonic approach: Ore Geology Reviews, v. 60, 174–190.

Burnham, C.W., 1979, Magmas and hydrothermal fluids, *in* Barnes, H.L., ed., Geochemistry of hydrothermal ore deposits, 2nd ed.: New York, Wiley, p. 71–136.

Cembrano, J., and Lara, L., 2009, The link between volcanism and tectonics in the southern volcanic zone of the Chilean Andes: A review: Tectonophysics, v. 471, p. 96–113.

Chelle-Michou, C., Rottier, B., Caricchi, L., and Simpson, G., 2017, Tempo of magma degassing and the genesis of porphyry copper deposits: Scientific Reports, v. 7, p. 1–12, no. 40566.

Chiaradia, M., 2014, Copper enrichment in arc magmas controlled by overriding plate thickness: Nature Geoscience, v. 7, p. 43– 46.

——2015, Crustal thickness control on Sr/Y signatures of recent arc magmas: An Earth scale perspective: Scientific Reports, v. 5, p. 1–5, no. 8115.

——2020a, How much water in basaltic melts parental to porphyry copper deposits?: Frontiers in Earth Science, v. 8, p. 138, doi: 10.3389/feart.2020.00138.

——2020b, Gold endowments of porphyry deposits controlled by precipitation efficiency: Nature Communications, v. 11, p. 1–10, no. 248.

Chiaradia, M., and Caricchi, L., 2017, Stochastic modelling of deep magmatic controls on porphyry copper deposit endowment: Scientific Reports, v. 7, p. 44523.

Chiaradia, M., Merino, D., and Spikings, R., 2009, Rapid transition to long-lived deep crustal magmatic maturation and the formation of giant porphyry-related mineralization (Yanacocha, Peru): Earth and Planetary Science Letters, v. 288, p. 505–515.

Chiaradia, M., Schaltegger, U., Spikings, R.A., Wotzlaw, J.F., and Ovtcharova, M., 2013, How accurately can we date the duration of magmatic-hydrothermal events in porphyry systems?: Economic Geology, v. 108, p. 565–584.

Chin, E.J., Shimizu, K., Bybee, G.M., and Erdman, M.E., 2018, On the development of the calc-alkaline and tholeiitic magma series: A deep crustal cumulate perspective: Earth and Planetary Science Letters, v. 482, p. 277–287.

Cline, J.S., and Bodnar, R.J., 1991, Can economic porphyry copper mineralization be generated by a "typical" calc-alkaline melt?: Journal of Geophysical Research, v. 96, p. 8113–8126.

Cooke, D.R., Hollings, P., and Walshe, J.L., 2005, Giant porphyry deposits: Characteristics, distribution, and tectonic controls: Economic Geology, v. 100, p. 801–818.

Core, D.P., Kesler, S.E., and Essene, E.J., 2006, Unusually Cu-rich magmas associated with giant porphyry copper deposits: Evidence from Bingham, Utah: Geology, v. 34, p. 41–44.

Cox, D., Watt, S.F.L., Jenner, F.E., Hastie, A.R., Hammond, S.J., and Kunz, B.E., 2020, Elevated magma fluxes deliver high-Cu magmas to the upper crust: Geology, v. 48, p. 957–960.

Defant, M.J., and Drummond, M.S., 1990, Derivation of some modern arc magmas by melting of young subducted lithosphere: Nature, v. 347, p. 662–665.

Du, J., and Audétat, A., 2020, Early sulfide saturation is not detrimental to porphyry Cu-Au formation: Geology, v. 48, doi: https://doi.org/10.1130/G47169.1.

Farner, M.J., and Lee, C.-T.A., 2017, Effects of crustal thickness on magmatic differentiation in subduction zone volcanism: A global study: Earth and Planetary Science Letters, v. 470, p. 96–107.

Gustafson, L.B., and Hunt, J.P., 1975, The porphyry copper deposit at El Salvador, Chile: Economic Geology, v. 70, p. 857–912.

Hedenquist, J.W., and Lowenstern, J.B., 1994, The role of magmas in the formation of hydrothermal ore deposits: Nature, v. 370, p. 519–527.

Jenner, F.E., O'Neill, H.St.C., Arculus, R.J., and Mavrogenes, J.A., 2010, The magnetite crisis in the evolution of arc-related magmas and the initial concentration of Au, Ag and Cu: Journal of Petrology, v. 51, p. 2445–2464.

Jensen, E.P., and Barton, M.D., 2000, Gold deposits related to alkaline magmatism: Reviews in Economic Geology, v. 13, p. 279–314.

Jugo, P., 2009, Sulfur content at sulfide saturation in oxidized magmas: Geology, v. 37, p. 415–418.

Hattori, K.H., and Keith, J.D., 2001, Contribution of mafic melt to porphyry copper mineralization: Evidence from Mount Pinatubo, Philippines, and Bingham Canyon, Utah, USA: Mineralium Deposita, v. 36, p. 799–806.

Kelley, K.A., and Cottrell, E., 2009, Water and the oxidation state of subduction zone magmas: Science, v. 325, p. 605–607.

Keith, J.D., Whitney, J.A., Hattori, K., Ballantyne, G.H., Christiansen, E.H., Barr, D.L., Cannan, T.M., and Hook, C.J., 1997, The role of magmatic sulfides and mafic alkaline magmas in the Bingham and Tintic mining district, Utah: Journal of Petrology, v. 38, p. 1679–1690.

Kesler, S.E., 1997, Metallogenic evolution of convergent margins: Selected ore deposit models: Ore Geology Reviews, v. 12, p. 153–171.

Lee, C.-T.A., and Tang, M., 2020, How to make porphyry copper deposits: Earth and Planetary Science Letters, v. 529, p. 1–11, no. 115868.

Lee, C.-T.A., Luffi, P., Chin, E.J., Bouchet, R., Dasgupta, R., Morton, D.M., Le Roux, V., Yin, Q., and Jin, D., 2012, Copper systematics in arc magmas and implications for crust-mantle differentiation: Science, v. 336, p. 64–68.

Li, Y., Selby, D., Condon, D., and Tapster, S., 2017, Cyclic magmatic-hydrothermal evolution in porphyry systems: High-precision U-Pb and Re-Os geochronology constraints on the Tibetan Qulong porphyry Cu-Mo deposit: Economic Geology, v. 112, p. 1419–1440.

Li, Y., Feng, L., Kiseeva, E.S., Gao, Z., Guo, H., Du, Z., Wang, F., and Shi, L., 2019, An essential role for sulfur in sulfide-silicate melt partitioning of gold and magmatic gold transport at subduction settings: Earth and Planetary Science Letters, v. 528, no. 1-12, no. 115850.

Lu, Y.J., Loucks, R.R., Fiorentini, M.L., Yang, Z.M., and Hou, Z.Q., 2015, Fluid flux melting generated post-collisional high-Sr/Y copper-ore-forming water-rich magmas in Tibet: Geology, v. 43, p. 583–586.

Loucks, R.R., 2014, Distinctive composition of copper-ore-forming arc magmas: Australian Journal of Earth Sciences, v. 61, p. 5–16.

Macpherson, C.G., Dreher, S.T., and Thirlwall, M.F., 2006, Adakites without slab melting: High pressure differentiation of island arc magma, Mindanao, The Philippines: Earth and Planetary Science Letters, v. 243, p. 581–593.

Matjuschkin, V., Blundy, J.D., and Brooker, R.A., 2016, The effect of pressure on sulphur speciation in mid- to deep-crustal arc magmas and implications for the formation of porphyry copper deposits: Contributions to Mineralogy and Petrology, v. 171, p. 1–25.

Mercer, C.N., Reed, M.H., and Mercer, C.M., 2015, Time scales of porphyry Cu deposit formation: Insights from titanium diffusion in quartz: Economic Geology, v. 110, p. 587–602.

Miyashiro, A., 1974, Volcanic rock series in island arcs and active continental margins: American Journal of Science, v. 274, p. 321–355.

Moss, R., Scott, S.D., and Binns, R.A., 2001, Gold content of Eastern Manus Basin volcanic rocks: Implications for enrichment in associated hydrothermal precipitates: Economic Geology, v. 96, p. 91–107.

Mungall, J.E., 2002, Roasting the mantle: Slab melting and the genesis of major Au and Au-rich Cu deposits: Geology, v. 30, p. 915–918.

Müntener, O., Kelemen, P.O., and Grove, T.L., 2001, The role of H_2O during crystallization of primitive arc magmas under uppermost mantle conditions and genesis of igneous pyroxenites: An experimental study: Contributions to Mineralogy and Petrology, v. 141, p. 643–658.

Murakami, H., Seo, J.H., and Heinrich, C., 2010, The relation between Cu/Au ratio and formation depth of porphyry-style Cu-Au ± Mo deposits: Mineralium Deposita, v. 45, p. 11–21.

Newman, S., and Lowenstern, J.B., 2002, VolatileCalc: A silicate melt-H_2O-CO_2 solution model written in Visual Basic for Excel: Computers and Geosciences, v. 28, p. 597–604.

O'Neill, H.St.C., and Mavrogenes, J.A., 2002, The sulfide capacity and the sulfur content at sulfide saturation of silicate melts at 1400°C and 1 bar: Journal of Petrology, v. 43, p. 1049–1087.

Plank, T., Kelley, K.A., Zimmer, M.M., Hauri, E.H., and Wallace, P.J., 2013, Why do mafic arc magmas contain ~4 wt % water on average?: Earth and Planetary Science Letters, v. 364, p. 168–179.

Perrin, A., Goes, S., Prytulak, J., Rondenay, S., and Davies, D.R., 2018, Mantle wedge temperatures and their potential relation to volcanic arc location: Earth and Planetary Science Letters, v. 501, p. 67–77, doi: 10.1016/j.epsl.2018.08.011.

Rabbia, O.M., Correa, K.J., Hernández, L.B., and Ulrich, T., 2017, "Normal" to adakite-like arc magmatism associated with the El Abra porphyry copper deposit, Central Andes, northern Chile: International Journal of Earth Sciences (Geologische Rundschau), v. 106, p. 2687–2711.

Reich, M., Parada, M.A., Palacios, C., Dietrich, A., Schultz, F., and Lehmann, B., 2003, Adakite-like signature of late Miocene intrusions at the Los Pelambres giant porphyry copper deposit in the Andes of central Chile: Metallogenic implications: Mineralium Deposita, v. 38, p. 876–885.

Rezeau, H., and Jagoutz, O., 2020, The importance of H_2O in arc magmas for the formation of porphyry Cu deposits: Ore Geology Reviews, v. 126, p. 104744, https://doi.org/10.1016/j.oregeorev. 2020.103744.

Richards, J.P., 2009, Postsubduction porphyry Cu-Au and epithermal Au deposits: Products of remelting of subduction-modified lithosphere: Geology, v. 37, p. 247–250.

——2011, High Sr/Y arc magmas and porphyry Cu ± Mo ± Au deposits: Just add water: Economic Geology, v. 106, p. 1075–1081.
——2013, Giant ore deposits formed by optimal alignments and combinations of geological processes: Nature Geoscience, v. 6, p. 911–916.
——2018, A shake-up in the porphyry world?: Economic Geology, v. 113, p. 1225–1233.
Richards, J.P., and Kerrich, R., 2007, Adakite-like rocks: Their diverse origins and questionable role in metallogenesis: Economic Geology, v. 102, p. 537–576.
Richards, S.W., and Holm, R.J., 2013, Tectonic preconditioning and the formation of giant porphyry deposits: Society of Economic Geologists Special Publication 17, p. 265–275.
Rintoul, M.D., and Torquato, S., 1997, Precise determination of the critical threshold and exponents in a three-dimensional percolation model: Journal of Physics A: Mathematical and General, v. 30, p. L585–L592.
Rock, N.M.S., and Groves, D.I., 1988, Do lamprophyres carry gold as well as diamonds?: Nature, v. 332, p. 253–255.
Rohrlach, B.D., and Loucks, R.R., 2005, Multi-million-year cyclic ramp-up of volatiles in a lower crustal magma reservoir trapped below the Tampakan Cu-Au deposit by Mio-Pliocene crustal compression in the southern Philippines, *in* Porter, T.M., ed., Super porphyry copper and gold deposits—a global perspective: Adelade, PGC Publishing, v. 2, p. 369–407.
Rosenbaum, G., Giles, D., Saxon, M., Betts, P.G., Weinberg, R.F., and Duboz, C., 2005, Subduction of the Nazca Ridge and the Inca Plateau: Insights into the formation of ore deposits in Peru: Earth and Planetary Science Letters, v. 239, p. 18–32.
Sillitoe, R.H., 1972, A plate tectonic model for the origin of porphyry copper deposits: Economic Geology, v. 67, p. 184–197.
——2000, Gold-rich porphyry deposits: Descriptive and genetic models and their role in exploration and discovery: Reviews in Economic Geology, v. 13, p. 315–345.
——2010, Porphyry copper systems: Economic Geology, v. 105, p. 3–41.
Sisson, T.W., and Grove, T.L., 1993, Experimental investigations of the role of H_2O in calc-alkaline differentiation and subduction zone magmatism: Contributions to Mineralogy and Petrology, v. 113, p. 143–166.
Stern, C.R., Skewes, M.A., and Arévalo, A., 2010, Magmatic evolution of the Giant El Teniente Cu-Mo deposit, Central Chile: Journal of Petrology, v. 52, p. 1591–1617.
Sun, W., Zhang, H., Ling, M.-X., Ding, X., Chung, S.-L-., Zhou, J., Yang, X.-Y., and Fan, W., 2011, The genetic association of adakites and Cu-Au ore deposits: International Geology Reviews, v. 53, p. 691–703.
Syracuse, E.M., van Keken, P.E., and Abers, G.A., 2010, The global range of subduction zone thermal models: Physics of the Earth and Planetary Interiors, v. 183, p. 73–90.
Takada, A., 1994, The influence of regional stress and magmatic input on styles of monogenetic and polygenetic volcanism: Journal of Geophysical Research, v. 99, p. 13563–13573.
Tang, M., Erdman, M., Eldridge, G., and Lee, C.-T.A., 2018, The redox "filter" beneath magmatic orogens and the formation of continental crust: Science Advances, v. 4, p. 1–7, no. eaar4444.
Tatsumi, Y., 1989, Migration of fluid phases and genesis of basalt magmas in subduction zones: Journal of Geophysical Research–Solid Earth, v. 94, p. 4697–4707.
Tosdal, R.M., and Richards, J.P., 2001, Magmatic and structural controls on the development of porphyry Cu ± Mo ± Au deposits: Reviews in Economic Geology, v. 14, p. 157–181.
Turner, S.J., and Langmuir, C.H., 2015, What processes control the chemical compositions of arc front stratovolcanoes?: Geochemistry Geophysics Geosystems, v. 16, p. 1865–1893.
Von Quadt, A., Erni, M., Martinek, K., Moll, M., Peytcheva, I., and Heinrich, C.A., 2011, Zircon crystallization and the lifetimes of ore-forming magmatic-hydrothermal systems: Geology, v. 39, p. 731–734.
Wallace, P.J., 2005, Volatiles in subduction zone magmas: Concentrations and fluxes based on melt inclusion and volcanic gas data: Journal of Volcanology and Geothermal Research, v. 140, p. 217– 240.
Wilkinson, J.J., 2013, Triggers for the formation of porphyry ore deposits in magmatic arcs: Nature Geoscience, v. 6, p. 917–925.

Massimo Chiaradia is senior lecturer at the Department of Earth Sciences of the University of Geneva (Switzerland). He obtained his M.Sc. degree at the University of Padova (Italy) and a Ph.D. from the University of Fribourg (Switzerland). His research focuses on the petrogenesis of arc magmas with implications for continental crust formation and the relationship between magma chemistry, dynamics of subduction zones and the formation of porphyry-type deposits. To carry out his research Massimo combines fieldwork with various analytical techniques including petrography and ore microscopy, mineral and rock geochemistry, light and heavy stable isotopes, radiogenic isotopes, and high-precision radiometric dating.